Eur. Phys. J. B **33**, 381–390 (2003)
DOI: 10.1140/epjb/e2003-00179-2

THE EUROPEAN PHYSICAL JOURNAL B

Normal state conduction in $Gd(Ba_{2-x}Pr_x)Cu_3O_{7+\delta}$

M.R. Mohammadizadeh and M. Akhavan[a]

Magnet Research Laboratory (MRL), Department of Physics, Sharif University of Technology, PO Box 11365-9161, Tehran, Iran

Received 12 January 2003 / Received in final form 8 April 2003
Published online 3 July 2003 –

Abstract. The normal state resistivity of single phase polycrystalline $Gd(Ba_{2-x}Pr_x)Cu_3O_{7+\delta}$ samples with $0.0 \leq x \leq 0.50$ have been investigated. There is a distinct metal-insulator transition at $x_c^{\rm MIT} = 0.2$ and a superconductor-insulator transition at $x_c^{\rm SIT} = 0.35$ with the increase of x. The two-dimensional variable range hopping is dominant in the normal state resistivity of the samples. The localization length, hopping range, and hopping energy of carriers show that Pr doping strongly localizes the carriers in normal state, and finally causes the suppression of superconductivity.

PACS. 74.25.Fy Transport properties (electric and thermal conductivity, thermoelectric effects, etc.) – 74.72.Bk Y-based cuprates – 71.30.+h Metal-insulator transitions and other electronic transitions

Introduction

The normal state of the high temperature cuprate superconductors shows many unusual properties, which are far from the standard Fermi liquid behavior. A typical anomalous property is the temperature dependence of the resistivity, which is linearly proportional to temperature T, in contrast with the T^2 dependence expected for a Fermi liquid; the optical conductivity, in contrast with the well known Drude theory, is roughly proportional to the inverse frequency. These indicate that the charge dynamics have a strongly incoherent character. Another example is the so-called pseudogap behavior observed in the underdoped region near the Mott insulating phase, which is a frequency threshold for the strong excitation of spin and charge modes [1].

Among high temperature superconductors (HTSC), the $PrBa_2Cu_3O_{7-\delta}$ (Pr-123) compound in the orthorhombic phase, in contrast with other $RBa_2Cu_3O_{7-\delta}$ (R-123) compounds (R=Y and rare earth elements), is an insulator [2]. Different anomalous effects have been observed when Pr atom is substituted in R-123 and other HTSC. For a recent review on the role of Pr in HTSC see reference [3]. Although, many attempts have been made to explain the insulating behavior of Pr-123, some groups have reported observation of superconductivity in the single crystal [4], powder, polycrystalline, and thin films of this compound [5]. It seems that the appearance of superconductivity in Pr-123 refers to its defective structure, which arises in highly non-equilibrium synthesis conditions allowing for locating the larger Ba atom at Pr position. Such conclusion has recently been reported for $Gd(Ba_{2-x}Pr_x)Cu_3O_{7+\delta}$ system [6] -in agreement with Tomkowicz [7], and also supported by the experimental study of Narozhnyi and Drechsler [8]. It has been believed for a long time that superconductivity suppression in the $R_{1-x}Pr_xBa_2Cu_3O_{7-\delta}$ system, caused by the hole localization and disappearance of superconductivity at $x_c = 0.3$–0.6 (depending on R), is associated with a metal-insulator transition (MIT) [9,10]. The nature of this localization has not been defined precisely, though many researchers have suggested the transition to be of the Anderson kind [11]. The conclusion that MIT occurs for all Pr-doped compounds, has been drawn based on the changes of character of the temperature dependence of electrical resistivity from metallic to semiconducting-like. However, the functional dependence of $\rho(T)$ curve with Pr concentration has not been systematically studied.

Among different models for describing the charge transport in materials, hopping conduction between localized states have been widely used for normal state of HTSC [12], semiconductors [13,14], perovskites [15], and quantum interfaces [16]. In hopping conduction, the temperature dependence of resistivity has been calculated for a number of different cases [17]. The best known examples for hopping conduction are due to Mott and Davis [18], and Shklovskii and Efros [13]. For these two cases, the temperature dependence of resistivity is

$$\rho(T) = \rho_0' \exp(T_0/T)^p, \tag{1}$$

where T_0 is a characteristic temperature, which will be discussed later, and

$$p = (n+1)/(n+D+1). \tag{2}$$

[a] e-mail: akhavan@sharif.edu

Here, D is the dimensionality of the hopping process, and n describes the energy dependence of DOS in the vicinity of Fermi energy $N(E_F)$, which behaves like

$$N(E_F) \sim |E - E_F|^n. \quad (3)$$

The ρ_0' is supposed to have weak temperature dependence so, it is considered to be a temperature-independent coefficient. For an energy-independent DOS ($n = 0$), this leads to a Mott-Davis variable range hopping (VRH) case of $p = 1/3$ in two dimensions (2D) and $p = 1/4$ in three dimensions (3D). Shklovskii and Efros have analyzed the case of low carrier concentration in doped semiconductors, where electrons interact *via* the unscreened Coulomb potential. This leads to a gap in DOS that is pinned to E_F (Coulomb gap (CG)). They have shown that $n = 1$ for 2D, whereas $n = 2$ for 3D. This leads to the same exponent $p = 1/2$ for 2D and 3D in equation (2). In addition, based on the localized states, Philips [19] has developed the quantum percolation theory to account for the normal state properties, including the temperature dependence of ρ_0' given by

$$\rho(T) = \rho_0 (T/T_0)^{2p} \exp(T_0/T)^p. \quad (4)$$

Now, ρ_0 is independent of T. The pre-exponential factor $\rho_0' = \rho_0 \exp(T/T_0)^{2p}$ should be considered explicitly for a more exact study [20].

From the experimental point of view, there are some reports, which show that VRH in 3D (3D-VRH) is a correct mechanism in the normal state conductivity of HTSC as discussed below. In polycrystalline $Gd_{1-x}Pr_xBa_2Cu_3O_{7-\delta}$ samples, the normal state resistivity for $x \geq 0.35$, using equation (4) follows a 3D-VRH mechanism, whereas for $x < 0.35$ it shows a CG mechanism behavior [21]. The 3D-VRH is shown to be the conduction mechanism in polycrystalline Pr-123 with 13 K $< T <$ 100 K [22], Pr-123 films with 4 K $< T <$ 123 K [23], $Pr_{1-x}Ca_x$-123 ceramics with 16 K $< T <$ 162 K [24], $Pr_{1+x}Ba_{2-x}Cu_3O_{7+\delta}$ solid solution with 20 K $< T <$ 300 K [25], polycrystalline $Pb_2(Sr_{3-x}La_x)Cu_3O_{8+\delta}$ samples with 4 K $< T <$ 170 K [26], La_2CuO_4 compound with 20 K $< T <$ 67 K [27], and $Bi_{1.7}Pb_{0.3}Sr_2(Ca_{1-x}Nd_x)Cu_2O_y$ with 84 K $< T <$ 300 K [28]. Moreover, in double layered perovskite $KLaNb_2O_7$ with Li intercalated, it is shown that 2D-VRH well describes the low temperature properties of the material in 1 K $< T <$ 125 K [29]. On the other hand, in single crystals of $Bi_2(Sr,Ca)_{n+1}(Cu_{1-x}Co_x)_nO_{8-\delta}$ with $0 < x < 0.26$, the form of ρ *versus* T behavior is not clearly VRH, but may be approaching the CG [30]. The *ab* resistivity of $PrBa_2(Cu_{2.8}Ga_{0.2})O_{7-\delta}$ thin film, grown by pulsed laser deposition with 110 K $< T <$ 325 K, shows the CG character for over three orders of magnitude [31]. Jiang *et al.* [32], have also obtained that CG is a much better regime for Pr-123 crystals. So, CG, 2D-VRH, and 3D-VRH have been reported for normal state resistivity of different HTSCs.

In most of the reports dealing with the hopping conduction mentioned above, the pre-exponent factor $(T/T_0)^{2p}$ is omitted, and a temperature independent prefactor ($\rho_0' = \rho_0$) has been supposed in the fitting processes. Moreover, different temperature domains have been used in finding the dominant conducting regime. In addition to the above drawbacks, different amounts of oxygen content in similar samples is the reason for the non-unique dominant resistivity regimes. So, to attain the real mechanism(s) of conduction, it requires to follow some definite guidelines. Therefore, in order to see if the VRH or CG conduction mechanism corresponds to Pr-doping, we have studied the normal state resistivity behavior of $Gd(Ba_{2-x}Pr_x)Cu_3O_{7+\delta}$ samples, paying special attention to the distinction between metal-insulator transition and superconductor-insulator transition (SIT).

Experimental details

The $Gd(Ba_{2-x}Pr_x)Cu_3O_{7+\delta}$ single phase polycrystalline samples with $x = 0.0$, 0.05, 0.1, 0.15, 0.2, 0.25, 0.3, 0.35, 0.4, 0.5, 0.6, 0.8, and 1.0 were synthesized by the standard solid state reaction technique. In accordance with the procedures followed in reference [33], appropriate amounts of Gd_2O_3, Pr_6O_{11}, $BaCO_3$, and CuO powders with %99.9 purity were mixed, ground, and calcined at 840 °C for 24 h in an air atmosphere. Calcination was repeated twice with intermediate grinding. Then powders were reground, pressed into pellets, and synthesized at 930 °C for 24 h in an oxygen atmosphere. The samples were cooled to 550 °C and retained under oxygen flow for 16 h. Finally, they were furnace cooled to room temperature. The oxygen content of the samples was determined by the iodometric titration technique within ±0.03 accuracy.

The SEM topography have been undertaken to determine the grain size and homogeneity of samples by JEOL-JXA-840 instrument. The XRD measurements have been done by a Philips PW-3710 powder diffractometer with Cu K_α radiation and $\lambda = 1.5406$ Å in room temperature. The XRD patterns have been analyzed by the Rietveld structure refinement method, using a modified version of the DBW3.2 program [34]. An ac four-probe method with $f = 33$ Hz and 10 mA current was used for the conductivity measurements of the samples within the temperature range of 10 to 300 K. The size of the samples was about $8 \times 3 \times 2$ mm^3. The electrical contacts were attached to the long side of the samples by silver paste. A Lake Shore-330 temperature controller with two Pt-100 resistors was used for measuring and controlling the temperature to within ±10 mK.

Results and discussion

The SEM topographs show a homogeneous granular structure with micrometer grain size. The XRD patterns show that the single phase of 123 structure has been formed, and no considerable impurity peaks are detectable. The complete structural refinement results have been presented elsewhere [6]. For $x \geq 0.6$, the XRD patterns indicate

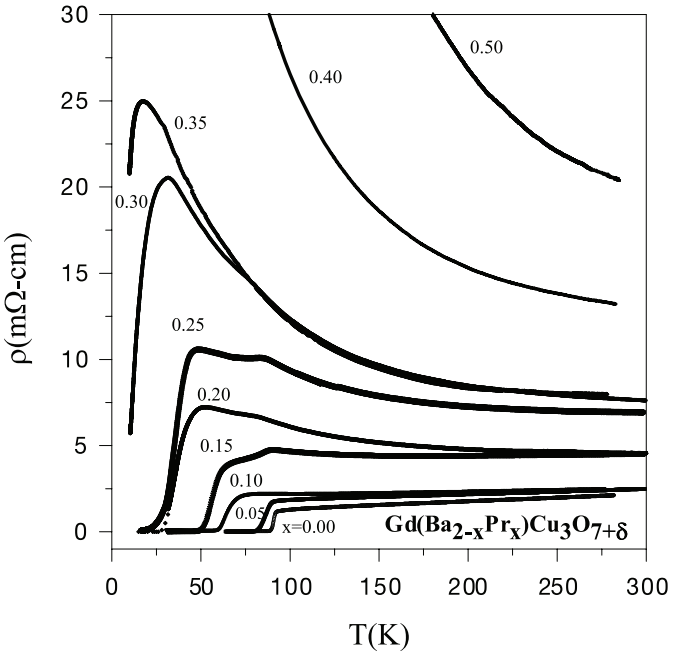

Fig. 1. Resistivity of the samples *versus* temperature for different amounts of Pr-doping (x).

that the 123 structure has not been formed. This is due to the solubility limit of R^{3+} at Ba^{2+} site, which is caused by the different charges and atomic sizes of Ba^{2+} and R^{3+} ions [35].

The resistivity data for $0.00 \leq x \leq 0.50$ samples are presented in Figure 1. With the increase of x, the superconducting transition temperature decreases and the width of transition temperature (ΔT_c) as well as the normal state resistivity increase with nearly the same amount of oxygen as given in Table 1. With the increase of the number of insulating parts in the grains (*i.e.* Pr substituted unit cells), the homogeneity of the grains decreases, which leads to larger ΔT_c. The normal state resistivity for $x < 0.2$ samples is metallic ($d\rho/dT > 0$), and for $x > 0.2$ is semiconducting-like ($d\rho/dT < 0$). So, within our 0.05 steps in samples preparation, the critical doping for MIT is $x_c^{\rm MIT} = 0.2$. In the metallic samples, the linear part of $\rho(T)$ from room temperature down to T_c, decreases with the increase of Pr doping. This corresponds to the doping dependence of the pseudogap, which is out of the scope of this paper, and has been discussed in reference [36].

In the samples with $x \leq 0.35$, the superconducting transition occurs, while for $x \geq 0.4$, there is no transition down to 10 K. Therefore, within our 0.05 steps in samples preparation, the critical doping for SIT is $x_c^{\rm SIT} = 0.35$. A SIT is also observed with application of magnetic field in $Gd(Ba_{2-x}Pr_x)Cu_3O_{7+\delta}$ system. It is important to distinguish the difference between critical x for SIT and MIT. The $x_c^{\rm SIT}$ in this system is less than the one for $(Gd_{1-x}Pr_x)Ba_2Cu_3O_{7-\delta}$ system (0.45) [37]. This means that the superconducting suppression by Pr at Ba site is more effective than Pr at R site. For the Pr at R site, we have an isovalent substitution of R^{3+} by Pr^{3+}, while in the Pr^{3+} at Ba^{2+} site, an effect on carrier density is expected due to different valency of Pr^{3+} and Ba^{2+}. This is also supported by Table 1, proving that valence variation is not balanced by the change of oxygen content. Another plausible explanation for this is that the Ba site is between the CuO_2 superconducting plane and Cu-O charge reservoir chains [38], which both have proved to be important in superconductivity of 123 systems. Hence, the existence of Pr atoms between these two correlated parts would be more destructive than at the R site, which is between the two independent CuO_2 planes.

Table 1. The superconducting transition temperature (T_c), the width of superconducting transition (ΔT_c), and oxygen contents of the samples for different amounts of Pr-doping (x).

x	$T_c(K)$	$\Delta T_c(K)$	$7+\delta$
0.00	90.84	2.0	6.99
0.05	86.63	6.5	7.03
0.10	63.69	8.2	7.03
0.15	55.69	10.0	7.09
0.20	44.50	12.5	7.01
0.25	39.02	11.6	7.06
0.30	23.01	18.0	7.06
0.35	10.0	25.0	6.97
0.40	—	—	6.99
0.50	—	—	6.96

We are interested to find the most correct conduction mechanism for the whole range of the normal state resistivity since, there is no evidence of any change in the conduction mechanism in the normal state with temperature variation. In other words, the lack of any special temperature or phase transition, implies that there should be a single dominant conduction mechanism in the normal state of these materials. Therefore, we will try to fit the $\rho(T)$ data within the framework of available proposed mechanisms and largest temperature range. Due to the large range of T in our fitting process, we have used the $\rho(T)$ with the explicit temperature dependent pre-exponent factor in equation (4) [20].

For the special $x = 0.15$, 0.20, 0.25, and 0.30 samples, as it is evident in Figure 1, a hump appears at about 80 K. This is an interesting new structural phase related to superconductivity in Pr-123 system [4], which has been discussed in details in reference [6]. It is concluded that no electronic phase difference exists in all the samples. By ignoring the anomalous parts from the resistivity curves of the corresponding samples, search for the dominant conduction mechanism has been carried out as follow.

In order to evaluate the normal state resistivity of the samples and judge on the probable effect of Pr on the normal state conduction, different models such as Anderson-Zou ($\rho = AT + B/T$) [39], thermally activated conduction ($\rho \sim \exp(T_0/T)$) [13], and semiconducting behavior ($\rho \sim \exp(-\Delta/T)$) [30] have been tested. None of these models show an appropriate fit for the whole range of Pr

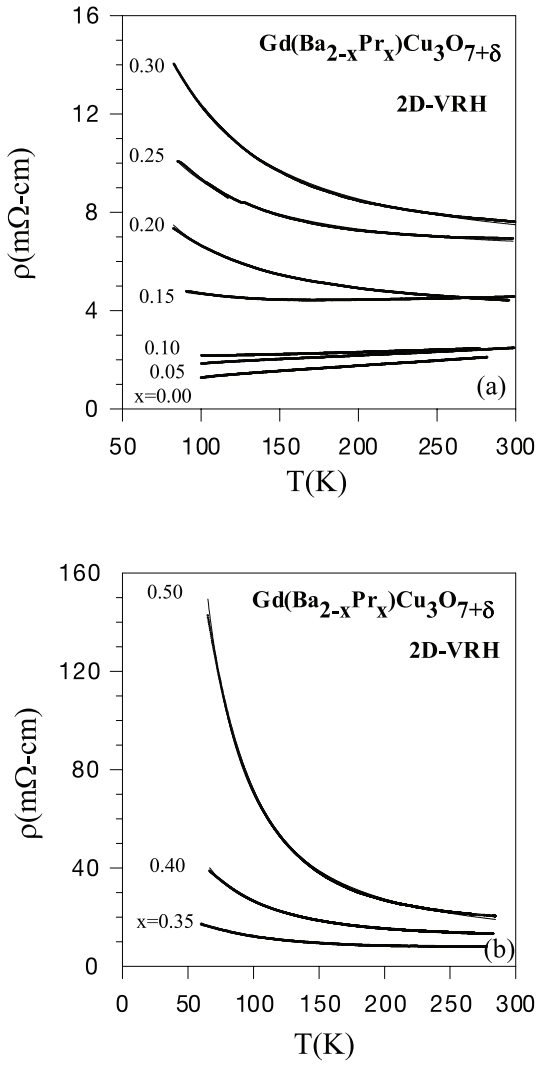

Fig. 2. The 2D-VRH fit (fixed-p method) for different amounts of Pr-doping (x). The dots appearing as a thick line are the experimental data, and the thin lines are the 2D-VRH regime predictions. (a): $0.00 \leq x \leq 0.30$, and (b): $0.35 \leq x \leq 0.50$.

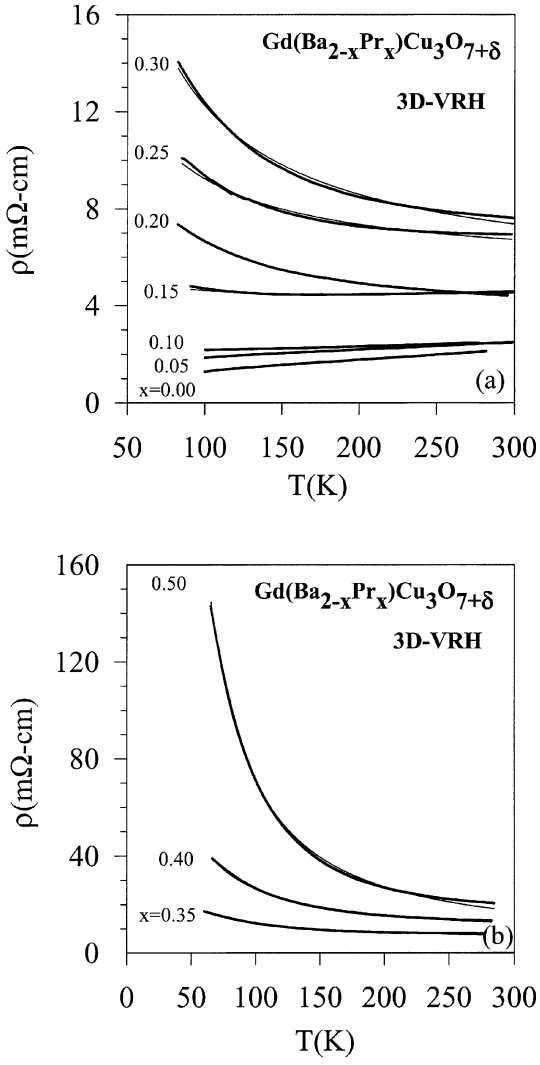

Fig. 3. The 3D-VRH fit (fixed-p method) for different amounts of Pr-doping (x). The dots appearing as a thick line are the experimental data, and the thin lines are the 3D-VRH regime predictions. (a): $0.00 \leq x \leq 0.30$, and (b): $0.35 \leq x \leq 0.50$.

doping. So, to test the VRH and CG regimes, we have fitted 2D-VRH, 3D-VRH, and CG regimes separately for all the samples with $0.0 \leq x \leq 0.50$ (*i.e.* fixed-p method). These results are shown in Figures 2 and 3. To recognize the best fit to the curves, the $\chi^2 s$ for the fits are also evaluated. The fitting results are shown in Table 2. It is evident that the numerical results for the 2D-VRH is more preferable than the others. It is to be noted that there are other reports in the literature, where the authors could not distinguish between the exact 2D-VRH or 3D-VRH mechanism in the normal state resistivity behavior, *i.e.* the insulating $Y_{0.37}Pr_{0.63}Ba_2Cu_3O_{7-\delta}$ [32], $Pr(SrBa)Cu_3O_{7-\delta}$ compound, in the 50 K $< T <$ 300 K range [40], or in the normal state resistivities ρ_c and ρ_{ab} of two twinned, fully-oxygenated single crystals of $PrBa_2Cu_3O_{7-\delta}$ and $Y_{0.47}Pr_{0.53}Ba_2Cu_3O_{7-\delta}$ [41].

Based on the results of the VRH and CG mechanisms by the fixed-p method in Table 2, the 2D-VRH is more valid. However, it would be interesting to leave the exponent value p as a variable, and obtain the valid regime automatically (*i.e.* the variable-p method). These results are presented in Figure 4 and Table 3. For almost all the samples, the value of p tends to 1/3 with a reasonable fit's results, which corresponds to the 2D-VRH. It is promising that this result is consistent with the above fixed-p method. The 2D behavior is the HTSC's well known character, which has been established for many years [42]. We have investigated the two dimensionality aspects of HTSC in comparison with the 2D electron gas system, which have been reviewed in reference [43].

It should also be mentioned that the theoretical assumption that has been used in deriving the exponent $p = 1/3$ and $1/4$ in the Mott-Davis case of equation (2) is the energy-independent DOS at Fermi energy, which may not be fulfilled for all HTSCs. So, the differences between the obtained exponent p and $1/3$ may be originated

Table 2. The resistivity fit in different modes for hopping conduction: 2D-VRH, 3D-VRH, and CG regimes for different amounts of Pr-doping (x). The ρ_0 and T_0 are the fit parameters and χ^2 shows the goodness of fit.

	3D-VRH($p = 1/4$)			2D-VRH($p = 1/3$)			CG($p = 1/2$)		
x	ρ_0(mΩ–cm)	T_0(K)	χ^2	ρ_0(mΩ–cm)	T_0(K)	χ^2	ρ_0(mΩ–cm)	T_0(K)	χ^2
0.00	0.02	0.03	0.9983	0.3	35	0.9991	0.6	167	0.9979
0.05	0.7	136	0.9953	0.9	313	0.9984	0.7	136	0.9953
0.10	1.1	811	0.9857	1.2	715	0.9987	1.1	812	0.9857
0.15	2.4	3229	0.7220	2.4	1500	0.9477	2.4	3229	0.7225
0.20	1.9	26224	0.9989	2.2	5105	0.9991	1.9	26224	0.9989
0.25	3.2	16802	0.9843	3.6	3912	0.9960	3.8	1077	0.9858
0.30	2.9	37391	0.9939	3.6	6407	0.9987	2.9	37392	0.9939
0.35	2.8	37870	0.9881	3.7	6018	0.9940	2.9	37871	0.9882
0.40	3.3	89812	0.9946	5.0	10909	0.9981	3.3	89813	0.9946
0.50	1.3	448583	0.9975	3.6	31272	0.9986	1.3	448583	0.9975

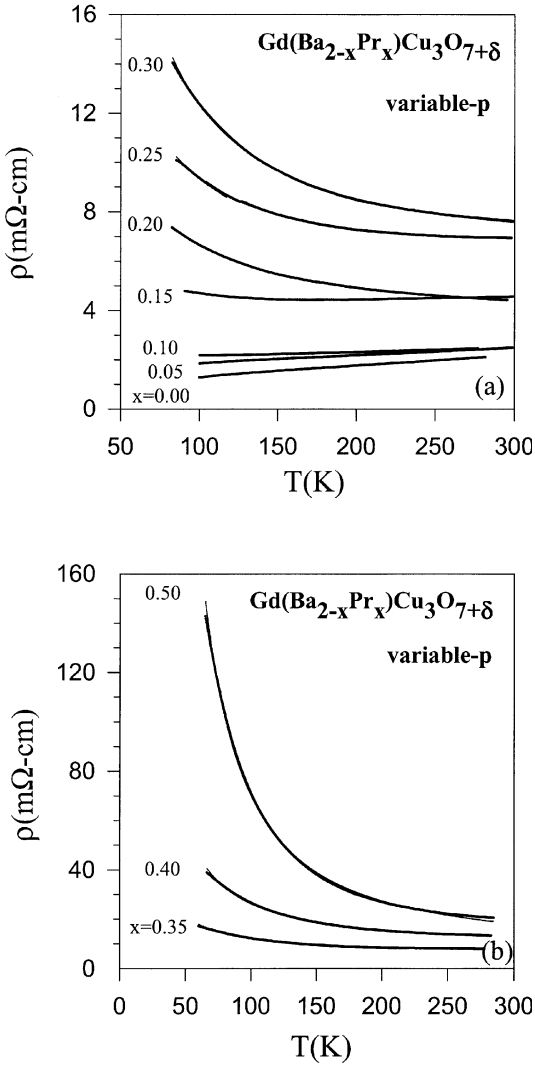

Fig. 4. Hopping conduction fit with the variable-p method for different amounts of Pr-doping (x). The dots appearing as a thick line are the experimental data and the thin lines are the hopping conduction predictions. (a): $0.00 \leq x \leq 0.30$, and (b): $0.35 \leq x \leq 0.50$.

Table 3. The resistivity fit with the variable-p method in hopping conduction for different amounts of Pr-doping (x). The ρ_0, T_0, and p are the fit parameters and χ^2 shows the goodness of fit.

x	ρ_0(mΩ–cm)	T_0(K)	p	χ^2
0.00	0.5	98	0.39	0.9994
0.05	1.0	349	0.37	0.9988
0.10	1.2	676	0.36	0.9998
0.15	2.4	1144	0.38	0.9902
0.20	2.1	9274	0.30	0.9998
0.25	3.7	2083	0.39	0.9994
0.30	3.8	3700	0.37	0.9995
0.35	3.9	4036	0.36	0.9945
0.40	5.4	7404	0.36	0.9983
0.50	3.4	38493	0.32	0.9986

from the later assumption. On the other hand, the VRH mechanism normally occurs in the low temperature region (below room temperature), where the energy is insufficient to excite the charge carriers across the CG. Hence, conduction takes place by hopping in small region ($\sim k_B T$) in the vicinity of E_F [44], where the DOS remains almost a constant. Of course, recent studies have shown that the VRH mechanism could also occur over a fairly large temperature range (100–900 K) [45]. Therefore, based on the present available approximate-theory, the non-zero DOS at Fermi energy (calculated for Gd-123 in reference [46] and other R-123 systems in [47]), and measured by the thermopower data in the 123 systems [48], we can consider a 2D-VRH behavior in the $Gd(Ba_{2-x}Pr_x)Cu_3O_{7+\delta}$ system. A definite conclusion requires exact experimental DOS data at Fermi level for HTSC, and development of the Mott-Davis localization theory for energy dependent DOS at E_F, which have not been yet performed.

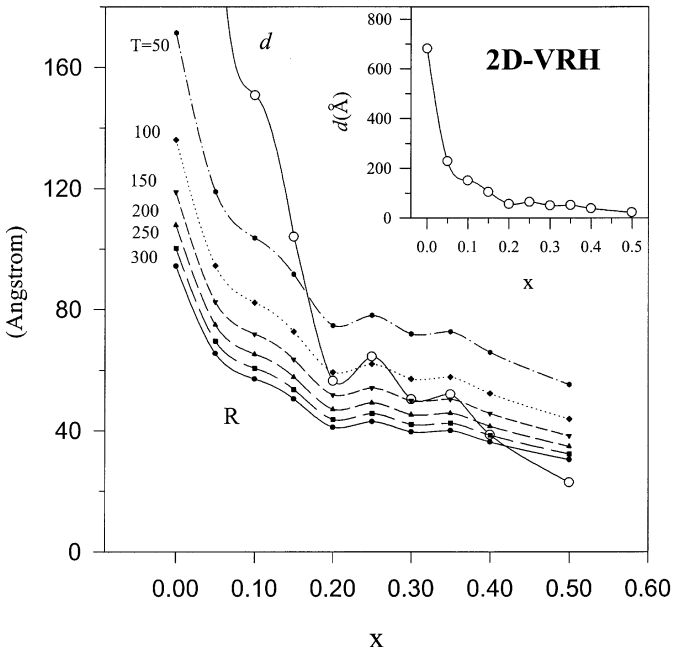

Fig. 5. The localization length (d) and hopping range (R) *versus* different amounts of Pr-doping (x), calculated from the results of the fixed-p method. The inset shows d *versus* x in the full range. The lines are guides to the eye.

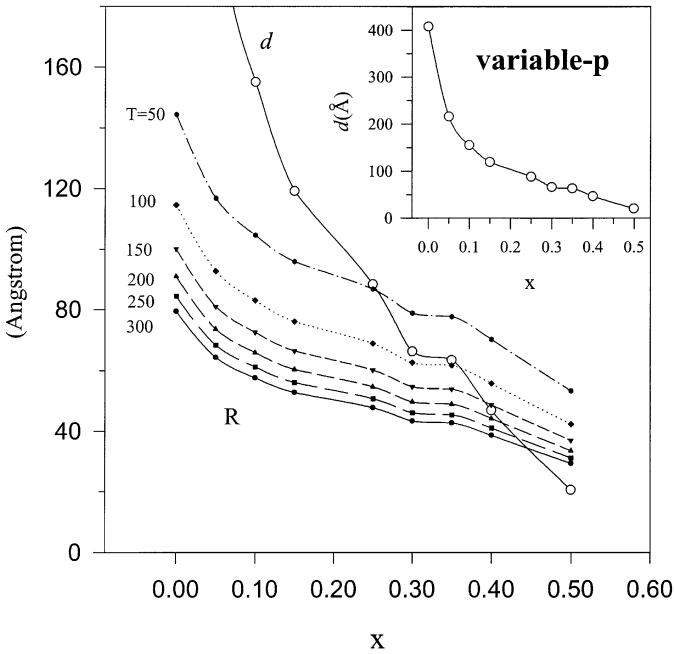

Fig. 6. The localization length (d) and hopping range (R) *versus* different amounts of Pr-doping (x), calculated from the results of the variable-p method. The inset shows d *versus* x in the full range. The lines are guides to the eye.

Using the Mott parameterization [18], the T_0 in equation (1) is related to the DOS at Fermi energy and the localization length of the carriers, as follow:

$$T_0^{2D} = 14/(k_B N_{2D}(E_F) d^2) \quad (5)$$

$$T_0^{3D} = 21/(k_B N_{3D}(E_F) d^3) \quad (6)$$

where d, the localization length, is the decay length of the localized wave function, $N(E_F)$ is the DOS at the Fermi energy, and k_B is the Boltzman constant. In 2D, the hopping energy (W), which the carriers need to hop over a distance R is [49]:

$$W_{2D} = 1/\left\{\pi R^2 N(E_F)\right\} \quad (7)$$

and the hopping range (R) is:

$$R_{2D} = \left[d/\left\{\pi N(E_F) k_B T\right\}\right]^{1/3}. \quad (8)$$

With the current estimate of $N(E_F) \approx 10^{21}$ states/(eV-cm^3) in 3D [50,51], and therefore, 10^{14} states/(eV-cm^2) [52], which is equivalent to 10^{-2} states/(eV-Å^2) in 2D, and the derived T_0 from fitting, the localization length, hopping range, and hopping energy can be achieved.

The localization length and hopping range for different amounts of Pr-doping are shown in Figure 5. The length of the localized wave functions is highest for Gd-123 ($x = 0.0$). This means that due to the very large d with respect to the distance of the neighboring atoms the overlap of the carriers' wave functions is enough for the conduction to perform easily. Further, by Pr-doping, the d decreases. With the increase of x, due to the decrease of localization length, the hopping range decreases too. This means that Pr-doping localizes the carriers in the normal state. When the localization length is very large, the extended carriers could do the conduction process easily. Therefore, for small x, the hopping range is less than the localization length. As we know, for VRH mechanism, R should be larger than d. So, in low temperatures *e.g.* 50 K, and for $x \geq 0.20$, the 2D-VRH occurs probably in the CuO_2 planes. With the increase of temperature, due to thermal fluctuations, hopping range decreases and the threshold of x (x_t), above which hopping occurs, changes; with the increase of temperature, x_t increases (Figs. 5 and 6).

The localization length has been calculated for different HTSC systems. Based on the I-V characteristic of planar-type junction specimens, it has been concluded that the localization length of Pr-123 films of 3000 Å thickness is 85 Å at 2K [52]. This is an evidence that the localization length is much larger than the size of the unit cell in 123 structures, in agreement with our results. However, in the bulk $Gd_{1-x}Pr_xBa_2Cu_3O_{7-\delta}$ system, d changes from 85 Å to 5 Å for $x = 0.0$ to 0.7, respectively [21]. The apparent discrepancy in the value of d for Pr-123 besides the fact that 2D-VRH has not been considered in [21], probably arises from the incompatibility of the data of films and bulk materials. This phenomenon has also been observed in the superconducting Tb-123 films [53] and insulating bulk Tb-123 compounds [54].

Figure 6 shows the localization length and hopping range for different x with variable-p method. Although, d and R have small differences in their values in comparison with the fixed-p method, their orders of magnitude

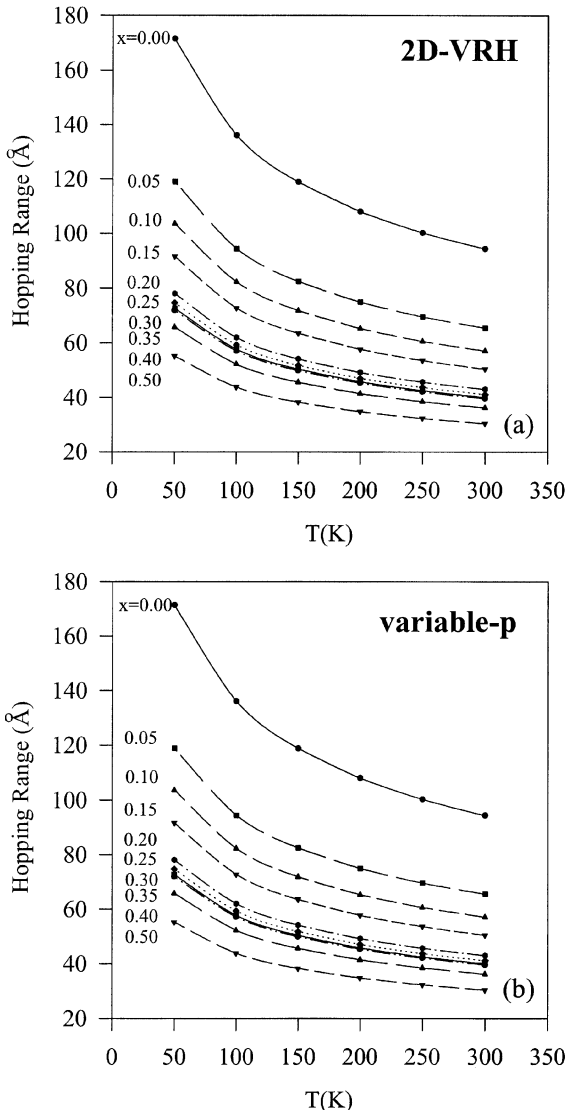

Fig. 7. The hopping range (R) *versus* temperature for different amounts of Pr-doping (x), calculated from the results of two methods (a): fixed-p, and (b): variable-p. The lines are guides to the eye.

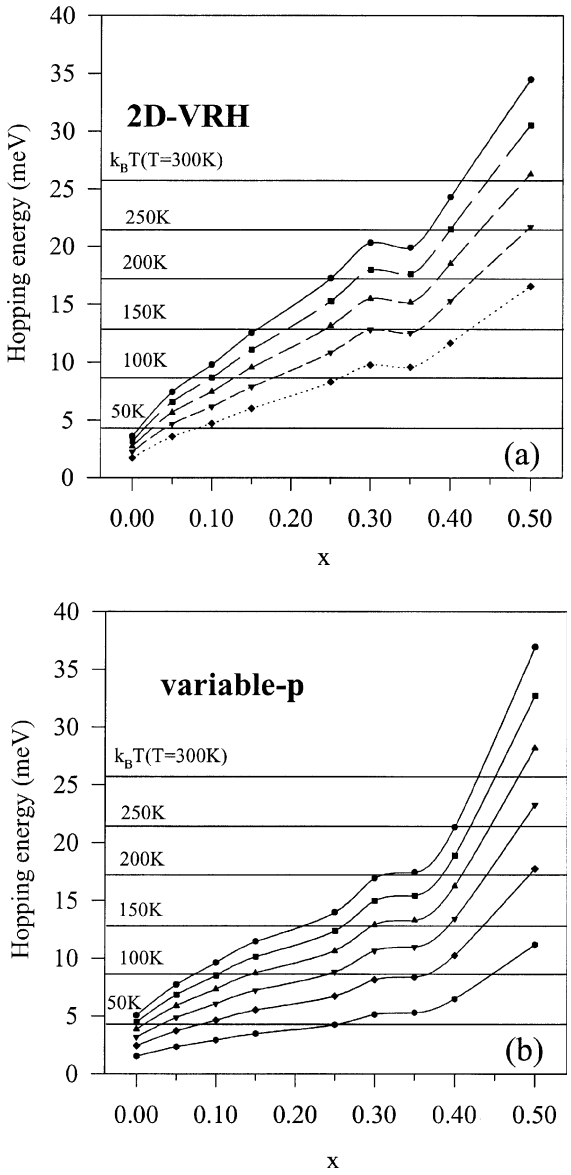

Fig. 8. The hopping energy (W) *versus* different amounts of Pr-doping (x) for different temperatures, calculated from the results of two method (a): fixed-p, and (b): variable-p. The lines are guides to the eye.

and changes with x and temperature are the same. This shows that the 2D-VRH, which has been resulted from the variable-p method, gives consistent T_0 with the fixed-p approach. The values of R *versus* temperature for both methods are presented in Figure 7. With the decrease of temperature, the thermal fluctuations decreases and hopping occurs also for larger distances. This results in the increase of R. This result is consistent with the values of hopping range *versus* temperature in perovskites [44]. Our results are also consistent with the hopping range in Pr-123, which is 960 Å at 2 K [52].

Figure 8 shows the hopping energy *versus* x for different temperatures with both fixed-p and variable-p methods. With the increase of Pr-doping, due to the destructive effect of Pr in conduction, the required energy of carriers for executing the hopping conduction increases. For performing VRH, the hopping energy should be larger than k_BT. In Figure 7, the horizontal lines show the k_BT for each temperature. For small temperatures, *e.g.* 50 K, due to small thermal fluctuations, small amount of hopping energy is enough to do hopping conduction. So, for $x \geq 0.20$, the VRH is a dominant mechanism of conduction in the normal state at $T = 50$ K. It is worthy to note that with the increase of temperature, x_t increases, which is exactly consistent with the extracted x_t from the hopping range curves. The results of both fixed-p and variable-p methods are also consistent with each other. In addition, Figure 9 shows the hopping energy *versus* temperature. With the increase of temperature, the hopping energy increases due to thermal fluctuations, which is destructive for hopping

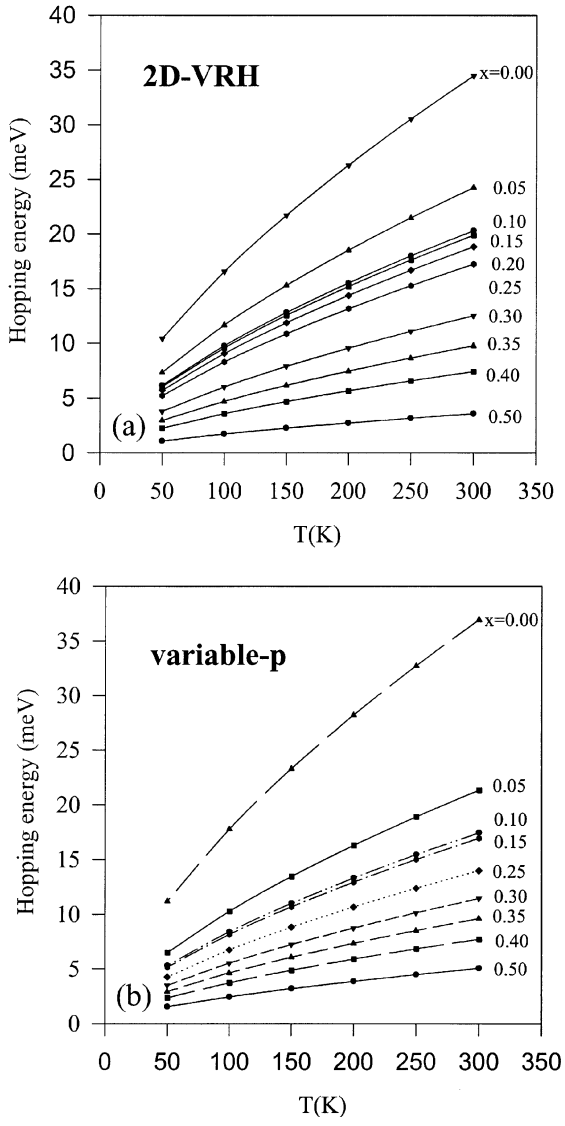

Fig. 9. The hopping energy (W) *versus* temperature for different amounts of Pr-doping (x), calculated from the results of two methods (a): fixed-p, and (b): variable-p. The lines are guides to the eye.

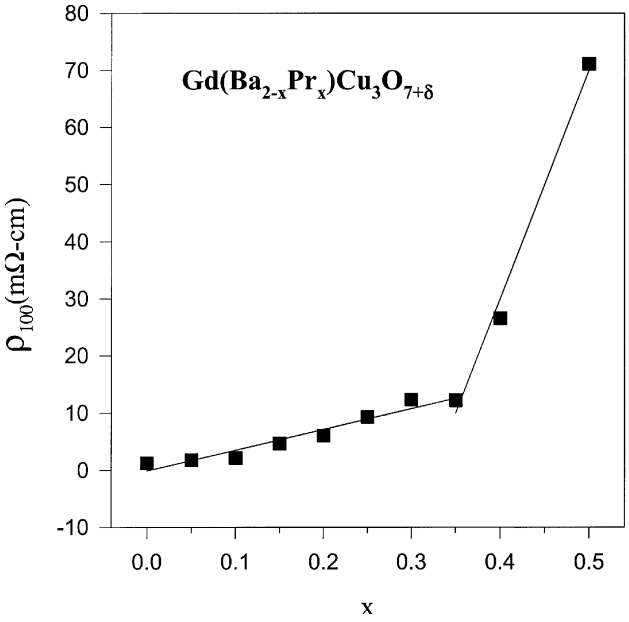

Fig. 10. Resistivity at $T = 100$ K *versus* different amounts of Pr-doping (x). The lines are linear fits.

conduction. This result is also consistent with the changes of hopping energy *versus* temperature in perovskites [44].

We have presented the resistivity at $T = 100$ K (ρ_{100}) *versus* x for all the samples in Figure 10. The ρ_{100} changes linearly in the $0.00 \leq x \leq 0.50$ range, but at $x > 0.35$ the slope of the line changes. This means that the normal state resistivity behaves differently depending on the samples' status, *i.e.* superconducting or non-superconducting. This is an important exhibition showing that the normal state of HTSC has inherent information on the superconducting state of the system.

It is worth noting that MIT does not necessarily occur at the concentration at which superconductivity disappears, as has been also emphasized by Tomkowicz *et al.* [11]. It is known that in some systems *e.g.* $Si_{1-x}Au_x$ [55], superconductivity is suppressed even before the occurrence of MIT. The opposite situation happens in most of the hole-doped HTSCs, as have been listed in Table 4. Different kind of samples: single crystals, polycrystallines, and thin films, with and without Pr-doping substitution at rare earth or Ba sites in 123 structure show MIT before SIT with doping. As the amounts of oxygen in our samples with different x remain constant (Tab. 1), the change of carriers doping in the CuO_2 superconducting planes should be due to the change in oxygen ordering, probable hybridization due to substitution, or others. Although, in some systems the MIT and SIT with x have been taken to be equivalent, such as in $La_{2-x}Sr_xCuO_4$ system [1], it seems that the distinction between them is a general rule, and the superposition of MIT and SIT should be viewed as a special case. Understanding the relation between MIT and SIT due to the elemental substitution in HTSCs needs more investigation.

Conclusions

We have studied the normal state resistivity *versus* temperature in $Gd(Ba_{2-x}Pr_x)Cu_3O_{7+\delta}$ system. There is a MIT at $x_c^{\rm MIT} = 0.20$ and a SIT at $x_c^{\rm SIT} = 0.35$. Distinction between MIT and SIT is a general rule, and their superposition is a special case. The appropriate conduction mechanism in the normal state is 2D-VRH. This dominant mechanism has been obtained with the fixed-p and variable-p methods. With the increase of Pr-doping, the hopping conduction is performed harder, and the localization length and hopping range decrease, while the hopping energy increases, consistent with d and R variations. Therefore, with Pr-doping, the normal state conduction is strongly affected. The localization of carriers in normal state with Pr-doping causes the suppression of

Table 4. Different compounds with different kinds of crystalline structures showing MIT and SIT values, with doping, including their references.

Compound	x_c^{MIT}	x_c^{SIT}	Sample	Reference
$Y_{1-x}Pr_xBa_2Cu_3O_{7-\delta}$	0.4	0.55	Polycrystalline	[56–58]
$Y_{1-x}Pr_xBa_2Cu_3O_{7-\delta}$	0.22	0.53	Single Crystal	[59]
$Y_{0.4}Pr_{0.6}Ba_{2-x}Sr_xCu_3O_{7-\delta}$	0.5	0.75	Polycrystalline	[60]
$Gd_{1-x}Pr_xBa_2Cu_3O_{7-\delta}$	0.3	0.4	Polycrystalline	[61,62]
$Sm_{1-x}Pr_xBa_2Cu_3O_{7-\delta}$	0.2	0.32	Polycrystalline	[51]
$Sm(Ba_{2-x}Pr_x)Cu_3O_{7+\delta}$	0.15	0.3	Polycrystalline	[63]
$Nd_{1-x}Pr_xBa_2Cu_3O_{7-\delta}$	0.25	0.35	Polycrystalline	[64]
$Nd_{1+x}Ba_{2-x}Cu_3O_{7+\delta}$	0.25	0.35	Polycrystalline	[64]
$Y_{1-x}Na_xBa_2Cu_3O_{7-\delta}$	0.2	0.5	Polycrystalline	[65]
$La_{1-x}Pr_xCaBaCu_3O_{7-\delta}$	0.5	0.7	Polycrystalline	[66]
$Bi_2(Pr_xCa_{3-x})Cu_3O_{8+\delta}$	0.5	0.6	Thin Film	[67]
$(La_{1-x}Pr_x)(Ba_{1.875}La_{0.125})Cu_3O_{7+\delta}$	0.17	0.22	Polycrystalline	[68]
$(Pb_{0.5}Ti_{0.5})Sr_2(Ca_{1-x}Pr_x)Cu_2O_z$	<0.35	0.6	Polycrystalline	[69]

superconductivity in Pr-doped systems. Finally, our results indicate evidences for strong correlations between normal and superconducting states in HTSCs.

The authors wish to thank M. Sedaghat. This work was supported in part by the Offices of Vice President for Research and Dean of Graduate Studies at Sharif University of Technology.

References

1. M. Imada, A. Fujimori, Y. Tokura, Rev. Mod. Phys. **70**, 1039 (1998)
2. M.R. Mohammadizadeh, H. Khosroabadi, M. Akhavan, Physica B **321**, 301 (2002); L. Soderholm, K. Zhang, D.G. Hinks, M.A. Beno, J.D. Jorgensen, C.U. Segre, I.K. Schuller, Nature **328**, 604 (1987)
3. M. Akhavan, Physica B **321**, 265 (2002)
4. Z. Zou, J. Ye, K. Oka, Y. Nishihara, Phys. Rev. Lett. **80**, 1074 (1998)
5. H.A. Blackstead, J.D. Dow, Solid State Commun. **115**, 137 (2000) and references therein
6. M.R. Mohammadizadeh, M. Akhavan, submitted to Phys. Rev. B (2002)
7. Z. Tomkowicz, Physica C **321**, 173 (1999)
8. V.N. Narozhnyi, S.-L. Drechsler, Phys. Rev. Lett. **82**, 461 (1999)
9. A. Kebede, C.S. Jee, J. Schwegler, J.E. Crow, T. Michalisin, G.H. Myer, R.E. Salomon, P. Schlottmann, M.V. Kuric, S.H. Bloom, R.P. Guertin, Phys. Rev. B **40**, 4453 (1989)
10. G. Niewa, S. Ghamaty, B.W. Lee, M.B. Maple, I.K. Schuller, Phys. Rev. B **44**, 6999 (1991); Z. Yamani, M. Akhavan, Phys. Stat. Sol. **162**, 157 (1997)
11. Z. Tomkowicz, P. Lunkenheimer, G. Knebel, M. Balanda, A.W. Pacyna, A.J. Zaleski, Physica C **331**, 45 (2000)
12. C. Quitmann, D. Andrich, C. Jarchow, M. Fleuster, B. Beschoten, G. Guntherodt, V.V. Moshchalkov, G. Mante, R. Manzke, Phys. Rev. B **46**, 11813 (1992)
13. B.I. Shklovskii, A.L. Efros, *Electronic Properties of Doped Semiconductors*, edited by M. Cardona, P. Fulde, H.-J. Queisser (Springer-Verlag, Berlin, 1984)
14. A.L. Efros, B.I. Shklovskii, J. Phys. C **8**, L49 (1975)
15. M.V. Lobanov, E.M. Kopnin, D. Xenikos, A.J. Grippa, E.V. Antipov, J.J. Capponi, M. Marezio, J.P. Julien, J.L. Tholence, Materials Research Bulletin **32**, 983 (1997)
16. D.M. Finlayson, J. Phys. Cond. Matt. **6**, 8277 (1994)
17. *Proceedings of the Fourth International Conference on Hopping and Related Phenomena, Marburg, 1991* [Philos. Mag. **65**, (1992)]
18. N.F. Mott, E.A. Davis, *Electronic Processes in Non-crystalline Materials*, 2nd edn. (Clarendon, Oxford, 1979)
19. J.C. Philips, Phys. Rev. B **38**, 5019 (1988); *ibid.* **41**, 850 (1990)
20. R. Mansfield, in: *Hopping Transport in Solids*, edited by M. Pollak, B.I. Shklovskii (North-Holland, Amsterdam, 1991)
21. Z. Yamani, M. Akhavan, Solid State Commun. **107**, 197 (1998).
22. B. Fisher, J. Genossar, L. Patlagan, G.M. Reisner, C.K. Subramaniam, A.B. Kaiser, Phys. Rev. B **50**, 4118 (1994)
23. M. Covington, L.H. Greene, Phys. Rev. B **62**, 12440 (2000)
24. M. Luszczek, Physica C **355**, 15 (2001)
25. W.H. Tang, J. Gao, Physica C **315**, 66 (1999)
26. H. Sasakura, K. Yoshida, K. Tagaya, S. Tsukui, M. Adachi, T. Oka, R. Oshima, Physica C **356**, 212 (2001)
27. B.I. Belevtsev, N.V. Dalakova, A.S. Panfilov, Physica C **282-287**, 1223 (1997)
28. S. Satyavathi, K.N. Kishore, V.H. Babu, O. Pena, Supercond. Sci. Technol. **6**, 93 (1996)
29. Y. Takano, S. Takayanagi, S. Ogawa, T. Yamadaya, N. Mori, Solid State Commun. **103**, 215 (1997)
30. Y.-K. Kuo, C.W. Schneider, D.T. Verebelyi, M.V. Nevitt, M.J. Skove, G.X. Tessema, H. Li, J.M. Pond, Physica C **319**, 1 (1999)
31. B. Leridon, A. Defossez, J. Dummont, J.P. Contour, Physica C **328**, 104 (1999)
32. W. Jiang, J.L. Peng, J.J. Hamilton, R.L. Greene, Phys. Rev. B **49**, 690 (1994)
33. Z. Yamani, M. Akhavan, Physica C **268**, 78 (1996)

34. D.B. Wiles, R.A. Young, J. Appl. Cryst. **14**, 149 (1981)
35. S. Li, E.A. Hayri, K.V. Ramanujachary, M. Greenblatt, Phys. Rev. B **38**, 2450 (1988)
36. M.R. Mohammadizadeh, M. Akhavan, Physica B (2003) (in press)
37. Z. Yamani, M. Akhavan, Phys. Rev. B **56**, 7894 (1997)
38. J.D. Jorgensen, B.W. Veal, A.P. Paulikas, L.J. Nowicki, G.W. Crabtree, H. Claus, W.K. Kwok, Phys. Rev. B **41**, 1863 (1990)
39. P.W. Anderson, Z. Zou, Phys. Rev. Lett. **60**, 132 (1988); M. Akhavan, Physica C **250**, 25 (1995)
40. A. Das, I. Zelenay, R. Suryanarayanan, Physica C **295**, 47 (1998)
41. G.A. Levin, T. Stein, C.N. Jiang, C.C. Almasan, D.A. Gajewski, S.H. Han, M.B. Maple, Physica C **282-287**, 1127 (1997); G.A. Levin, T. Stein, C.C. Almasan, S.H. Han, D.A. Gajewski, M.B. Maple, Phys. Rev. Lett. **80**, 841 (1998)
42. P.B. Littlewood, C.M. Varma, Phys. Rev. B **45**, 12636 (1992)
43. M.R. Mohammadizadeh, M. Akhavan, accepted for publication in Supercond. Sci. Technol. (2003)
44. W.-H. Jung, Physica B **304**, 75 (2001)
45. V. Ponnambalam, U.V. Varadaraju, Phys. Rev. B **42**, 8764 (1990)
46. G.Y. Guo, W.M. Temmerman, Phys. Rev. B **41**, 6372 (1990)
47. H. Khosroabadi, M.R. Mohammadizadeh, M. Akhavan, Physica C, **370**, 85 (2002); H. Khosroabadi, M.R. Mohammadizadeh, M. Akhavan, Physica B **321**, 360 (2002)
48. A.P. Gonçalves, I.C. Santos, E.B. Lopes, R.T. Henriques, M. Almeida, M.O. Figueiredo, Phys. Rev. B **37**, 7476 (1988)
49. V. Ambegaokar, B.I. Halperin, J.S. Langer, Phys. Rev. B **4**, 2612 (1971)
50. M.A. Kastner, R.J. Birgeneau, C.Y. Chen, Y.M. Chiang, D.R. Gabbe, H.P. Jenssen, T. Junk, C.J. Peters, P.J. Picone, T. Thio, T.R. Thurston, H.L. Tuller, Phys. Rev. B **37**, 111 (1988); C.S. Jee, A. Kebede, D. Nichols, J.E. Crow, T. Mihalisin, G.H. Myer, I. Perez, R.E. Salomon, P. Schlottmann, Solid State Commun. **69**, 379 (1989)
51. S.K. Malik, C.V. Tomy, P. Bhargava, Phys. Rev. B **44**, 7042 (1991)
52. U. Kabasawa, Y. Tarutani, M. Okamoto, T. Fukazawa, A. Tsukamoto, M. Hiratani, K. Takagi, Phys. Rev. Lett. **70**, 1700 (1993)
53. C.R. Fincher, Jr., G.B. Blanchet, Phys. Rev. Lett. **67**, 2902 (1991)
54. K.N. Yang, B.W. Lee, M.B. Maple, S.S. Laderman, Appl. Phys. A **46**, 229 (1988)
55. T. Furubayashi, N. Nishida, M. Yamaguchi, K. Morigaki, H. Ishimoto, Solid State Commun. **55**, 513 (1985)
56. M.B. Maple, B.W. Lee, J.J. Neumeier, G. Nieva, L.M. Paulius, C.L. Seaman, J. Alloys Compounds **181**, 135 (1992)
57. U. Neukirch, C.T. Simmons, P. Sladeczek, C. Laubschat, O. Strebel, G. Kaindl, D.D. Sarma, Europhys. Lett. **5**, 567 (1988)
58. V.E. Gasumyants, E.V. Vladimirskaya, I.B. Patrina, Phys. Solid State **39**, 1352 (1997)
59. C.N. Jiang, A.R. Baldwin, G.A. Levin, T. Stein, C.C. Almasan, D.A. Gajewski, S.H. Han, M.B. Maple, Phys. Rev. B **55**, R3390 (1997)
60. G. Cao, Y. Qian, X. Li, Z. Chen, C. Wang, K. Ruan, Y. Qiu, L. Cao, Y. Ge, Y. Zhang, J. Phys. Cond. Matt. **7**, L287 (1995)
61. H.D. Yang, P.F. Chen, C.R. Hsu, C.W. Lee, C.L. Li, C.C. Peng, Phys. Rev. B **43**, 10568 (1991)
62. Z. Yamani, M. Akhavan, Supercond. Sci. Technol. **10**, 427 (1997)
63. V.E. Gasumyants, M.V. Elizarova, R. Suryanarayanan, Phys. Rev. B **61**, 12404 (2000)
64. H. Iwasaki, J. Sugawara, N. Kobayashi, Physica C **185-189**, 1249 (1991)
65. Y. Dalichaouch, M.S. Torikachvili, E.A. Early, B.W. Lee, C.L. Seaman, K.N. Yang, H. Zhou, M.B. Maple, Solid State Commun. **65**, 1001 (1988)
66. C. Infante, M.K.E. Mously, R. Dayal, M. Husain, S.A. Siddiqi, P. Ganguly, Physica C **167**, 640 (1990)
67. K. Yoshida, H. Sasakura, S. Tsukui, R. Oshima, T. Santoh, Y. Mizokawa, Phys. Rev. B **61**, 11332 (2000)
68. D.B. Mitzi, P.T. Feffer, J.M. Newsam, D.J. Webb, P. Klavins, A.J. Jacobson, A. Kapitulnik, Phys. Rev. B **38**, 6667 (1988)
69. H.K. Lee, Physica B **284-288**, 1095 (2000)